Journal of Intelligent and Robotic Systems **22:** 315–330, 1998.

Feedback Control of an Omnidirectional Autonomous Platform for Mobile Service Robots

KEIGO WATANABE and YAMATO SHIRAISHI
Department of Mechanical Engineering, Saga University, 1-Honjomachi, Saga 840, Japan

SPYROS G. TZAFESTAS
Computer Science Division, National Technical University of Athens, Zografou Campus, 15773 Athens, Greece

JUN TANG
Department of Mechanical Engineering, Yamaguchi University, 2557 Tokiwadai, Ube 755, Japan

TOSHIO FUKUDA
Department of Micro Systems Engineering, Nagoya University, Furo-cho, Chikusa-ku, Nagoya 464, Japan

(Received: 6 December 1997; in final form: 30 January 1998)

Abstract. This paper proposes a feedback control scheme for an omnidirectional holonomic autonomous platform, which is equipped with three lateral orthogonal-wheel assemblies. Firstly, the dynamic properties of the platform are studied, and a dynamic model suitable for the application of control is derived. The control scheme constructed is of the resolved-acceleration type, with PI and PD feedback. The control scheme was experimentally applied to an actual mobile robotic platform. The results obtained show that full omnidirectionality can be achieved with decoupled rotational and translational motions. Omnidirectionality is one of the principal requirements for mobile robots designed for health-care and other general-hospital services.

Key words: omnidirectional mobile platform, omnidirectional mobile robot, holonomic robot, mobile service robot, omnidirectional-robot dynamic model, resolved acceleration feedback control.

1. Introduction

Mobile robots and manipulators mounted on mobile platforms are useful in a large variety of indoor service applications: industrial, medical and domestic. A partial list of environments where mobile service robots can assist ill, disabled and elderly people is: hospitals and clinics, dormitories for handicaped and elderly people, and sheldered workshops for physically disabled people. Three fundamental requirements of such service robots are:

- maneuvrability,
- safety for people and machines,
- manipulability and dexterity.

To meet the above requirements at a sufficient functional level, a synergetic fusion of several methodologies and technologies is needed, including control, sensing and artificial intelligence technologies.

A major recent advancement towards the achievement of high and safe maneuvrability is the development and use of omnidirectional mobile platforms/robots, instead of conventional platforms and robots with two independent driving wheels, or with the front-wheel handling and rear-wheel driving.

Omnidirectional mobile robots have been studied by using a variety of mechanisms. In particular, an holonomic vehicle has a full omnidirectionality with simultaneous and independently controlled rotational and translation motion capabilities. Several omnidirectional platforms have been known to be realized by driving wheel with steering (or offset driving wheel) [1, 2, 3], universal wheels [4, 5], spherical tires [6], or crawler mechanisms [7, 8].

A new family of holonomic wheeled platforms has also been proposed by Pin and Killough [9], in which an orthogonal-wheel concept has been introduced. It should be noted, however, that the conventional studies on the omnidirectional vehicles have been focused on the development of mechanisms or only on the analysis of kinematics, and hence there are little studies on the development of dynamic models and highly accurate control systems.

In this paper, we introduce one dynamic model for an omnidirectional mobile robot, in which it is assumed that the platform is based on three orthogonal-wheel assemblies. Then, to develop a control system with high performance for such a mobile robot, a resolved acceleration control system can be shown to be designed using such a dynamic model. The practical experiments are presented to illustrate the full omnidirectionality of the platform with decoupled rotational and translational motions.

2. Omnidirectional Mobile Platform with Orthogonal Wheels

In this section, we assume that the omnidirectional mobile robot platform consists of the orthogonal-wheel assembly mechanism proposed by Pin and Killough [9].

The basic lateral orthogonal-wheel assembly is illustrated in Figure 1. The major components are two spheres of equal diameter which have been sliced to resemble wide, i.e., rounded-tire wheels. The axle of each wheel is perpendicular to the sliced surfaces and is mounted using ball bearing so that the wheel is free-wheeling around its axle. Through a bracket which is holding the extremities of the wheel axle, each wheel can be driven to roll on its portion of spherical surface, rotating around an axis Z, perpendicular to the wheel axle. When these axes Z_1 and Z_2 are maintained parallel and at a constant distance from each other, and when the wheel rotations around these axes are synchronized, contact with the ground can be assured by at least one wheel, while allowing enough space for the brackets holding the wheel axles to clear the ground. These assemblies can be constructed

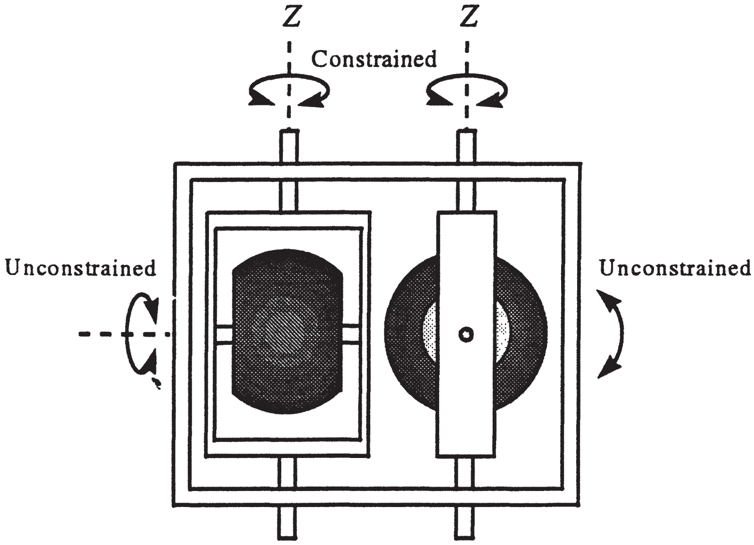

Figure 1. The lateral orthogonal-wheel assembly.

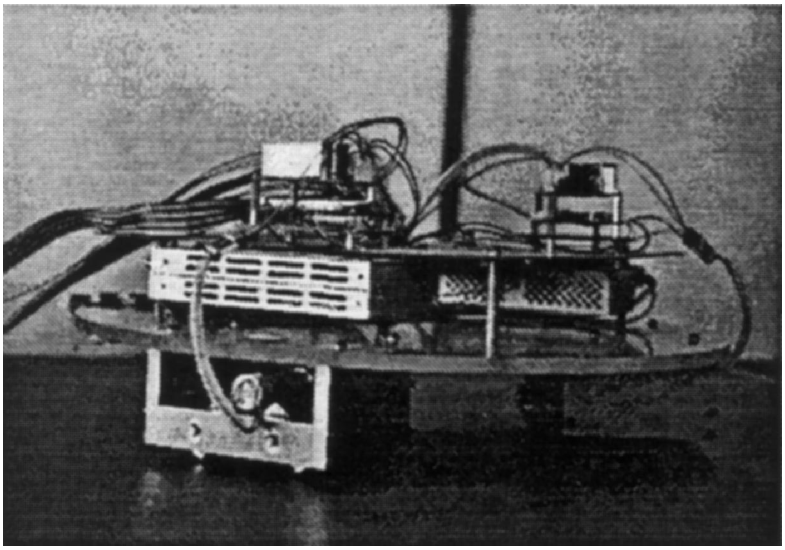

Figure 2. The appearance of an omnidirectional mobile platform.

by using more than two wheels, in which each wheel axle should be allocated with less than 90° offset.

In the following, it is assumed that a platform is based on three assemblies allocated at an equal distance from the center of gravity (c.g.) for the robot, in which one assembly consists of two wheels. The actual experimental mobile robot is shown in Figure 2.

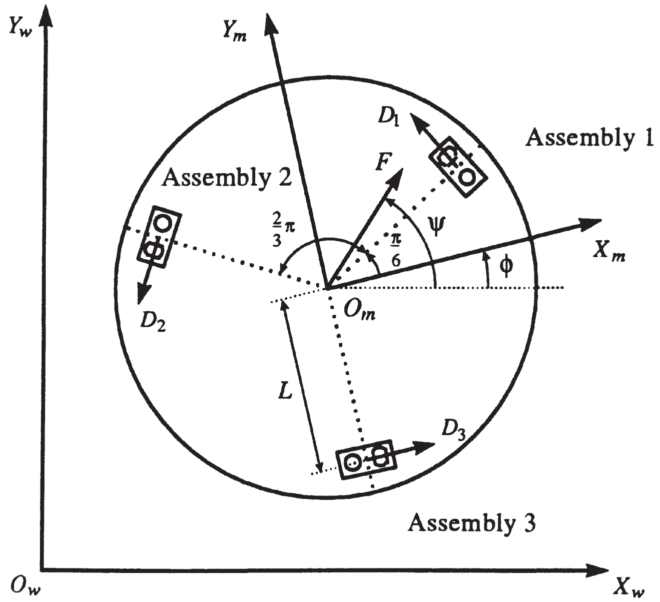

Figure 3. Model of an omnidirectional mobile robot.

3. Dynamic Model of the Omnidirectional Mobile Platform

Let the mobile robot be rigid moving on the work space. It is assumed that the absolute coordinate system $O_w : X_w Y_w$ is fixed on the plane and the moving coordinate system $O_m : X_m Y_m$ is fixed on the c.g. for the mobile robot as shown in Figure 3.

When defining the position vector of the c.g. for the mobile robot such as $\boldsymbol{S}_w = [x_w \; y_w]^{\mathrm{T}}$, we have

$$\boldsymbol{M}\ddot{\boldsymbol{S}}_w = \boldsymbol{F}_w, \tag{1}$$

where $\boldsymbol{F}_w = [F_x \; F_y]^{\mathrm{T}}$ is the force vector in the absolute coordinate system applied to the center of gravity of the mobile robot and $\boldsymbol{M}$ is a symmetric positive-definite matrix as $\boldsymbol{M} = \mathrm{diag}(M, M)$ with the mass M.

Let ϕ denote the angle between X_w- and X_m-coordinates, i.e., the rotational angle of the moving coordinate system with respect to the absolute coordinate system. When introducing the coordinate transformation matrix from the absolute coordinate system to the moving coordinate system such as

$$^{w}R_m = \begin{bmatrix} \cos\phi & -\sin\phi \\ \sin\phi & \cos\phi \end{bmatrix} \tag{2}$$

it follows that

$$\dot{\boldsymbol{S}}_w = {}^{w}R_m \dot{\boldsymbol{s}}_m, \tag{3}$$

$$\boldsymbol{F}_w = {}^{w}R_m \boldsymbol{f}_m, \tag{4}$$

where $\boldsymbol{s}_m = [x_m \;\, y_m]^{\mathrm{T}}$ and $\boldsymbol{f}_m = [f_x \;\, f_y]^{\mathrm{T}}$ are the position vector of the c.g. and the force vector applied to the c.g. in the moving coordinate system, respectively.

Therefore, transforming Equation (1) to the moving coordinate system gives

$$\boldsymbol{M}\left({}^{w}R_m^{\mathrm{T}}\,{}^{w}\dot{R}_m\dot{\boldsymbol{s}}_m + \ddot{\boldsymbol{s}}_m\right) = \boldsymbol{f}_m. \tag{5}$$

Then, the dynamic properties of the mobile robot can be described as [10]:

$$M\left(\ddot{x}_m - \dot{y}_m\dot{\phi}\right) = f_x, \tag{6}$$
$$M\left(\ddot{y}_m - \dot{x}_m\dot{\phi}\right) = f_y, \tag{7}$$
$$I_v\ddot{\phi} = M_I, \tag{8}$$

where I_v is the moment of inertia for the robot, M_I is the moment around the c.g. for the robot, and f_x, f_y, M_I are given by:

$$f_x = -\frac{1}{2}D_1 - \frac{1}{2}D_2 + D_3, \tag{9}$$
$$f_y = \frac{\sqrt{3}}{2}D_1 - \frac{\sqrt{3}}{2}D_2, \tag{10}$$
$$M_I = (D_1 + D_2 + D_3)L. \tag{11}$$

In addition, the driving system property [11] for each assembly is assumed to be given by

$$I_w\dot{\omega}_i + c\omega_i = ku_i - rD_i, \quad i = 1, 2, 3, \tag{12}$$

where L is the distance between any assembly and the c.g. of the robot; c is the viscous friction factor of the wheel; D_i is the driving force for each assembly; r is the radius of the wheel; I_w is the moment of inertia of the wheel around the driving shaft; ω_i is the rotational rate of the wheel; k is the driving gain factor; and u_i is the driving input torque.

On the other hand, the geometrical relationships among variables $\dot{\phi}$, $\dot{x}_m$, $\dot{y}_m$, and ω_i, i.e., the inverse kinematics are given by:

$$r\omega_1 = -\frac{1}{2}\dot{x}_m + \frac{\sqrt{3}}{2}\dot{y}_m + L\dot{\phi}, \tag{13}$$
$$r\omega_2 = -\frac{1}{2}\dot{x}_m - \frac{\sqrt{3}}{2}\dot{y}_m + L\dot{\phi}, \tag{14}$$
$$r\omega_3 = \dot{x}_m + L\dot{\phi}. \tag{15}$$

Therefore, using Equations (6)–(15) gives:

$$\ddot{x}_m = a_1\dot{x}_m + a_2'\dot{y}_m\dot{\phi} - b_1(u_1 + u_2 - 2u_3), \tag{16}$$
$$\ddot{y}_m = a_1\dot{y}_m - a_2'\dot{x}_m\dot{\phi} + \sqrt{3}b_1(u_1 - u_2), \tag{17}$$
$$\ddot{\phi} = a_3\dot{\phi} + b_2(u_1 + u_2 + u_3), \tag{18}$$

where

$$
\begin{aligned}
a_1 &= -3c/\big(3I_w + 2Mr^2\big), \qquad a_2' = 2Mr^2/\big(3I_w + 2Mr^2\big),\\
a_3 &= -3cL^2/\big(3I_w L^2 + I_v r^2\big),\\
b_1 &= kr/\big(3I_w + 2Mr^2\big), \qquad b_2 = krL/\big(3I_w L^2 + I_v r^2\big).
\end{aligned}
$$

It is easy to find that combining Equations (2), (3), (16) and (17) yields the appropriate dynamic equations in the absolute coordinate system for the robot. Thus, defining the state variable for the robot as $\boldsymbol{x} = [x_w\ y_w\ \phi\ \dot{x}_w\ \dot{y}_w\ \dot{\phi}]^{\mathrm{T}}$, the manipulated variable as $\boldsymbol{u} = [u_1\ u_2\ u_3]^{\mathrm{T}}$, and the output variable as $\boldsymbol{y} = [\dot{x}_w\ \dot{y}_m\ \phi]^{\mathrm{T}}$ yields the following state equation:

$$
\begin{aligned}
\dot{\boldsymbol{x}} &= A(\boldsymbol{x})\boldsymbol{x} + B(\boldsymbol{x})\boldsymbol{u}, &\quad (19)\\
\boldsymbol{y} &= C\boldsymbol{x}, &\quad (20)
\end{aligned}
$$

where

$$
A(\boldsymbol{x}) = \begin{bmatrix}
0 & 0 & 0 & 1 & 0 & 0\\
0 & 0 & 0 & 0 & 1 & 0\\
0 & 0 & 0 & 0 & 0 & 1\\
0 & 0 & 0 & a_1 & -a_2\dot{\phi} & 0\\
0 & 0 & 0 & a_2\dot{\phi} & a_1 & 0\\
0 & 0 & 0 & 0 & 0 & a_3
\end{bmatrix},
$$

$$
B(\boldsymbol{x}) = \begin{bmatrix}
0 & 0 & 0\\
0 & 0 & 0\\
0 & 0 & 0\\
b_1\beta_1 & b_1\beta_2 & 2b_1\cos\phi\\
b_1\beta_3 & b_1\beta_4 & 2b_1\sin\phi\\
b_2 & b_2 & b_2
\end{bmatrix}, \qquad
C = \begin{bmatrix}
0 & 0 & 0 & 1 & 0 & 0\\
0 & 0 & 0 & 0 & 1 & 0\\
0 & 0 & 1 & 0 & 0 & 0
\end{bmatrix},
$$

$$
\begin{aligned}
a_2 &= 1 - a_2' = 3I_w/\big(3I_w + 2Mr^2\big),\\
\beta_1 &= -\sqrt{3}\sin\phi - \cos\phi, \qquad \beta_2 = \sqrt{3}\sin\phi - \cos\phi,\\
\beta_3 &= \sqrt{3}\cos\phi - \sin\phi, \qquad \beta_4 = -\sqrt{3}\cos\phi - \sin\phi.
\end{aligned}
$$

Let the translational velocity of the robot in the absolute coordinate system be $V = (\dot{x}_w^2 + \dot{y}_w^2)^{1/2}$ and the azimuth of the robot in the absolute coordinate system be $\psi = \theta + \phi$. Here, θ denotes the angle between X_m-coordinate and $\boldsymbol{f}_m$, i.e., the azimuth of the robot in the moving coordinate system. Then, it is found that

$$
\begin{aligned}
\dot{x}_w &= V\cos\psi, &\quad (21)\\
\dot{y}_w &= V\sin\psi, &\quad (22)\\
\psi &= \arctan\frac{\dot{y}_w}{\dot{x}_w}, &\quad (23)
\end{aligned}
$$

where note that a counterclockwise rotation denotes the positive direction for the rotational motion of the robot.

It should be noted that X_w- and Y_w-directional motions in (19) are coupled, because the equation of motions is derived in the absolute coordinate system. However, since the rotational angle of the robot can be assured as $\phi = \psi - \theta$ even if the azimuth of the robot is changed arbitrarily, the mobile robot can realize a translational motion without changing the pose.

4. Resolved Acceleration Control

Since the dynamic equation is finally considered in the absolute coordinate system, solving Equation (19) with respect to u_i, $i = 1, 2, 3$, gives the following resolved acceleration control:

$$\begin{aligned} u_1 &= \frac{\beta_1(\ddot{x}_w^* - a_1\dot{x}_w + a_2\dot{\phi}\dot{y}_w)}{6b_1} \\ &\quad + \frac{\beta_3(\ddot{y}_w^* - a_1\dot{y}_w - a_2\dot{\phi}\dot{x}_w)}{6b_1} + \frac{\ddot{\phi}^* - a_3\dot{\phi}}{3b_2}, \end{aligned} \tag{24}$$

$$\begin{aligned} u_2 &= \frac{\beta_2(\ddot{x}_w^* - a_1\dot{x}_w + a_2\dot{\phi}\dot{y}_w)}{6b_1} \\ &\quad + \frac{\beta_4(\ddot{y}_w^* - a_1\dot{y}_w - a_2\dot{\phi}\dot{x}_w)}{6b_1} + \frac{\ddot{\phi}^* - a_3\dot{\phi}}{3b_2}, \end{aligned} \tag{25}$$

$$\begin{aligned} u_3 &= \frac{\cos\phi(\ddot{x}_w^* - a_1\dot{x}_w + a_2\dot{\phi}\dot{y}_w)}{3b_1} \\ &\quad + \frac{\sin\phi(\ddot{y}_w^* - a_1\dot{y}_w - a_2\dot{\phi}\dot{x}_w)}{3b_1} + \frac{\ddot{\phi}^* - a_3\dot{\phi}}{3b_2}, \end{aligned} \tag{26}$$

where $\ddot{x}_w^*$, $\ddot{y}_w^*$ and $\ddot{\phi}^*$ are given by adding PI-servo or PD-servo to $\ddot{x}_{w\mathrm{d}}$, $\ddot{y}_{w\mathrm{d}}$ and $\ddot{\phi}_\mathrm{d}$ such that

$$\ddot{x}_w^* = \ddot{x}_{w\mathrm{d}} + K_{\dot{x}\mathrm{p}}e_{\dot{x}} + K_{\dot{x}\mathrm{i}}\int_0^t e_{\dot{x}}\,\mathrm{d}t, \tag{27}$$

$$\ddot{y}_w^* = \ddot{y}_{w\mathrm{d}} + K_{\dot{y}\mathrm{p}}e_{\dot{y}} + K_{\dot{y}\mathrm{i}}\int_0^t e_{\dot{y}}\,\mathrm{d}t, \tag{28}$$

$$\ddot{\phi}^* = \ddot{\phi}_\mathrm{d} + K_{\phi\mathrm{v}}\dot{e}_\phi + K_{\phi\mathrm{p}}e_\phi. \tag{29}$$

Here, $K_{\cdot\mathrm{p}}$ is the proportional gain, $K_{\cdot\mathrm{i}}$ is the integral gain, $K_{\cdot\mathrm{v}}$ is the derivative gain, and each error is defined by:

$$e_{\dot{x}} = \dot{x}_{w\mathrm{d}} - \dot{x}_w, \tag{30}$$

$$e_{\dot{y}} = \dot{y}_{w\mathrm{d}} - \dot{y}_w, \tag{31}$$

$$e_\phi = \phi_\mathrm{d} - \phi, \tag{32}$$

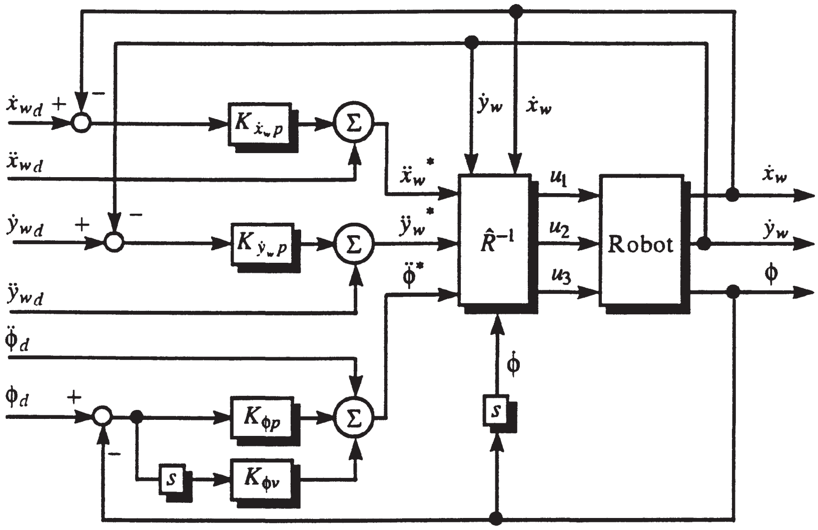

Figure 4. A resolved acceleration control system.

where $\dot{x}_{w\mathrm{d}}$, $\dot{y}_{w\mathrm{d}}$ and ϕ_{d} denote the references for $\dot{x}_w$, $\dot{y}_w$ and ϕ, respectively. It should be noted that the solutions u_i, $i = 1, 2, 3$, exist for all t, because the input distribution factors b_1 and b_2 are always nonzero constants. The block diagram of a resolved acceleration control system for the mobile robot is shown in Figure 4, in which $\widehat{R}^{-1}$ denotes the estimated inverse dynamic model.

5. Experimental Results

We have applied the above control system to an actual mobile robot. It was assumed that the control sampling period is 50 ms and the total experimental time is 20 s. The physical parameters of the mobile robot are as follows:

$$\begin{aligned} I_{\mathrm{v}} &= 11.25\,\mathrm{kgm}^2, \quad I_w = 0.02108\,\mathrm{kgm}^2, \quad c = 5.983 \times 10^{-6}\,\mathrm{kgm}^2/\mathrm{s}, \\ M &= 9.4\,\mathrm{kg}, \quad L = 0.178\,\mathrm{m}, \quad r = 0.0245\,\mathrm{m}, \quad k = 1.0. \end{aligned}$$

It was also assumed that the initial moving coordinate system is equal to the absolute coordinate system, and the initial value of state variable is given as $\boldsymbol{x} = [0\;0\;0\;0\;0\;0]^{\mathrm{T}}$.

5.1. SIMULTANEOUSLY TRANSLATIONAL AND ROTATIONAL MOTIONS

The omnidirectional mobile robot can independently achieve the translational motion and the rotational motion around the c.g. in the two-dimensional plane. To check this property, the holonomic property, it was assumed that the robot must travel with a fixed azimuth angle $\psi_{\mathrm{d}} = \pi/4$ rad for 20 s, but with zero rotational angle for 0–10 s and with a uniformly varying rotational angle from $\phi_{\mathrm{d}} = 0$ rad to

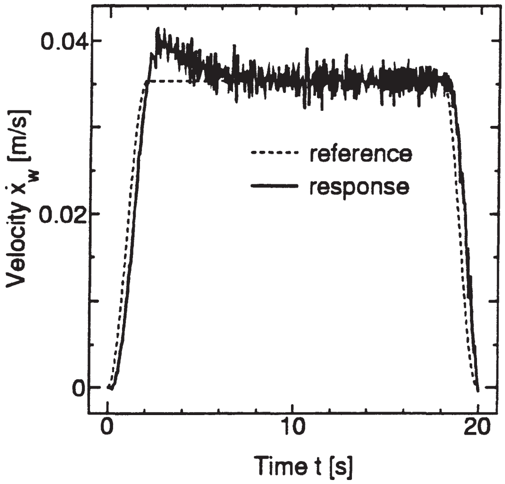

Figure 5. Velocity $\dot{x}_w$ for Case 1.

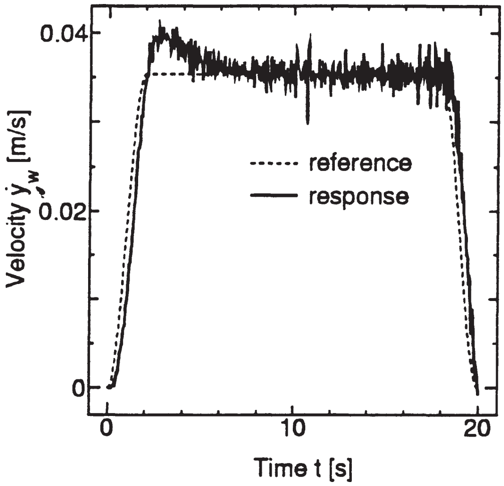

Figure 6. Velocity $\dot{y}_w$ for Case 1.

$\phi_\mathrm{d} = \pi/2$ rad for 10–20 s. Although the moving velocity was to be $V_\mathrm{d} = 0.05$ m/s in the steady-state, a sinusoidal reference velocity was set for each 2 seconds at the starting and ending duration.

Using these V_d and ψ_d, the corresponding $\dot{x}_{w\mathrm{d}}$ and $\dot{y}_{w\mathrm{d}}$ were derived from (21) and (22), and $\ddot{x}_{w\mathrm{d}}$ and $\ddot{y}_{w\mathrm{d}}$ were also derived by their derivatives.

5.1.1. *Case 1*

Figures 5–7 show the results for the case when the servo gains are given as in Table I. In this case, it is found that the control of ϕ is achieved very well, while the velocity control results have an overshoot.

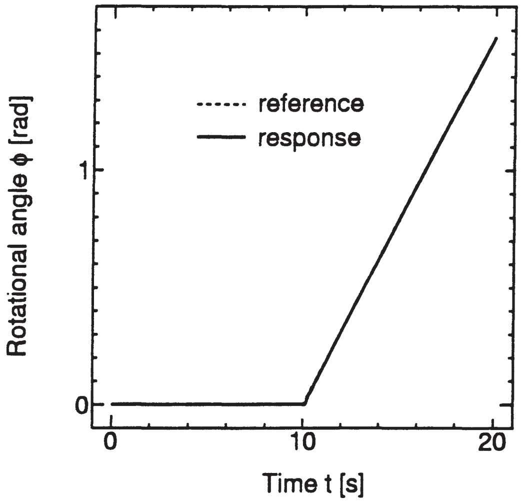

Figure 7. Rotational angle ϕ for Case 1.

Table I. Gains for Case 1

$K_{\phi p}$	$K_{\phi v}$	$K_{\dot{x} i}$	$K_{\dot{x} p}$	$K_{\dot{y} i}$	$K_{\dot{y} p}$
2.25	3.0	1.0	2.0	1.0	2.0

Table II. Gains for Case 2

$K_{\phi p}$	$K_{\phi v}$	$K_{\dot{x} i}$	$K_{\dot{x} p}$	$K_{\dot{y} i}$	$K_{\dot{y} p}$
2.25	3.0	25.0	10.0	25.0	10.0

5.1.2. *Case 2*

To improve the responses on $\dot{x}_w$ and $\dot{y}_w$, adjusted servo gains are tabulated in Table II. The corresponding control results are shown in Figures 8–13. It is found from these figures that a good trajectory control result is obtained, though there exist successive oscillations in the velocity responses. This seems to be attributed to the reason that the dc-servo-driver has a restricted resolution ability.

5.2. CIRCULAR MOTION WITH A FIXED POSE

As a motion that a conventional mobile robot cannot achieve, we can consider a circular motion with a radius of curvature less than half of the distance between wheels, that is, its motion has a center of rotation on the distance between wheels. The omnidirectional mobile robot, of course, can easily achieve such a motion. In

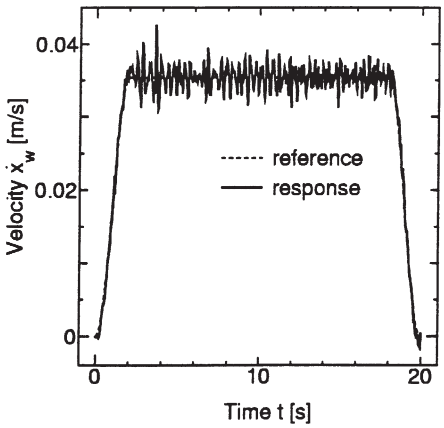

Figure 8. Velocity $\dot{x}_w$ for Case 2.

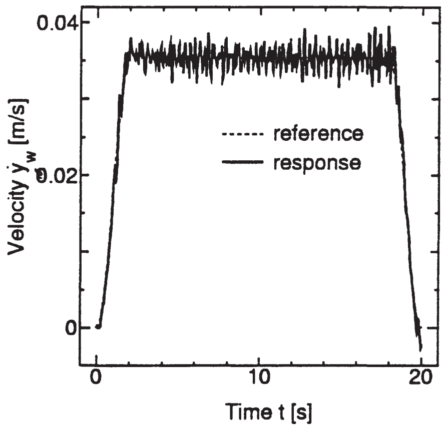

Figure 9. Velocity $\dot{y}_w$ for Case 2.

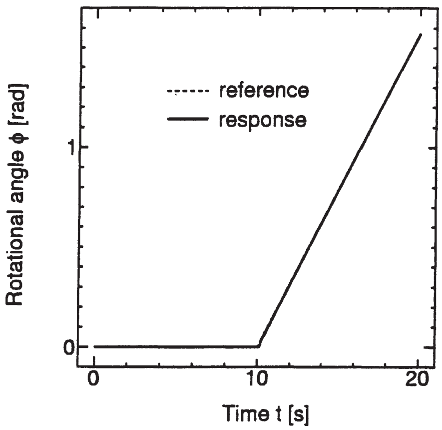

Figure 10. Rotational angle ϕ for Case 2.

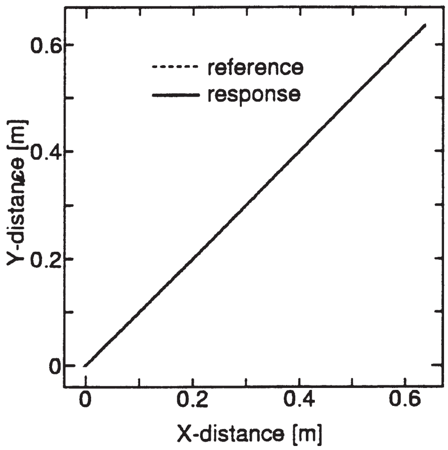

Figure 11. Trajectory for Case 2.

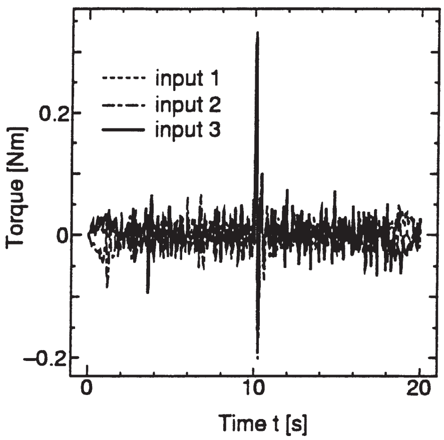

Figure 12. Input torque for Case 2.

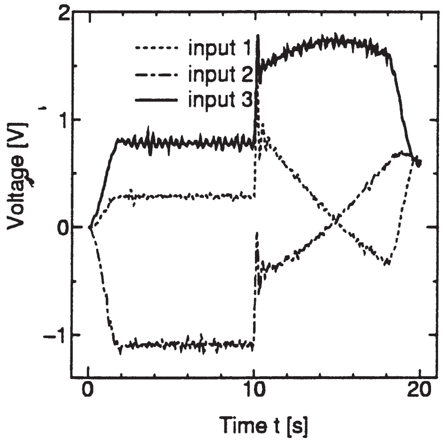

Figure 13. Input voltage for Case 2.

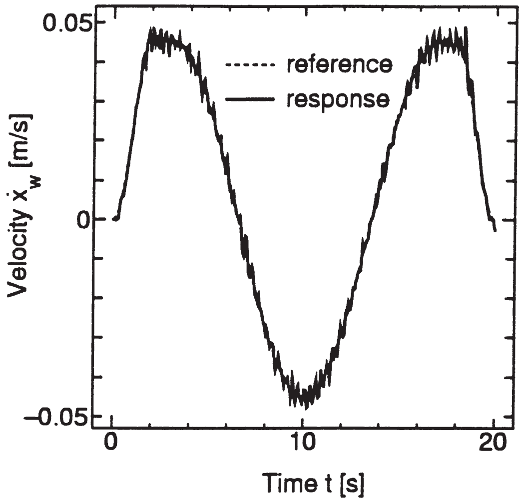

Figure 14. Velocity $\dot{x}_w$ for a circular path.

the following experiment, it was assumed that a circular trajectory has a radius of curvature 0.1 m, while the distance between wheels is 0.356 m. The resultant moving velocity was given by $V_\mathrm{d} = 0.04488$ m/s, but a sinusoidal reference velocity was set for each 2 seconds at the starting and ending duration. The moving azimuth was $\psi_\mathrm{d} = 0.0$ rad for each 3 seconds at the starting and ending duration, while it had a uniformly successive increment up to 2π rad for the remaining 14 seconds, where the robot pose, the rotational angle was fixed as $\phi_\mathrm{d} = 0.0$ rad for the whole duration.

The corresponding control results are shown in Figures 14–19, where the servo gains are the same as those tabulated in Table II. From these figures, it is seen that satisfactory control results are obtained without changing the servo gains.

5.3. 8 CHARACTER MOTION WITH A SIMULTANEOUS ROTATION

In this section, the following 8 character path was considered to check the tracking performance of the robot for the case when the references $\dot{x}_{w\mathrm{d}}$ and $\dot{y}_{w\mathrm{d}}$ are changed frequently, and to examine the effect of a time-varying ϕ on the responses.

It was assumed that $V_\mathrm{d} = 0.05$ m/s, but with an acceleration and deceleration for each 2 seconds at the starting and ending duration. The 8 character was composed of two squared path, where there existed an acceleration and deceleration for 1 second at each corner. The resultant path was symmetry with respect to the x-coordinate. It was also assumed that the reference rotational angle was zero for 0–10 s, while it was uniformly time-increasing from $\phi_\mathrm{d} = 0$ rad to $\phi_\mathrm{d} = \pi/2$ rad for 10–20 s.

The control results are shown in Figures 20–22, where the servo gains given in Table II were used. It is understood from these figures that some overshoots appear

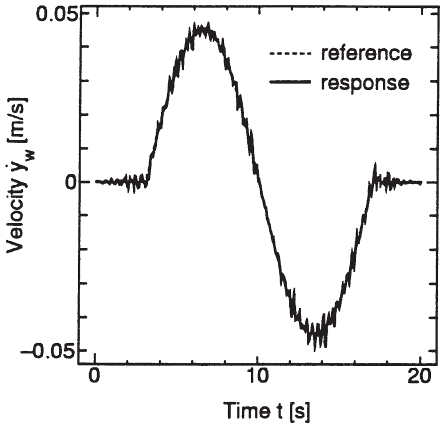

Figure 15. Velocity $\dot{y}_w$ for a circular path.

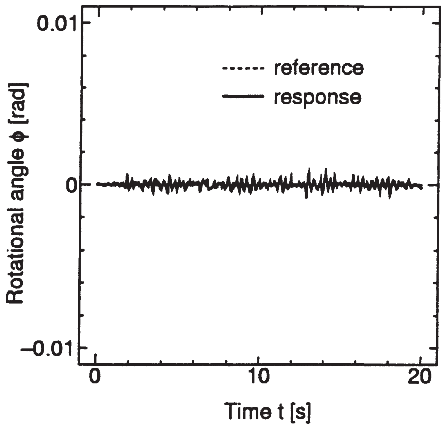

Figure 16. Rotational angle ϕ for a circular path.

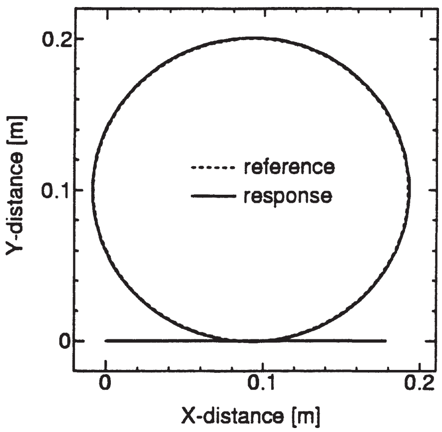

Figure 17. Trajectory for a circular path.

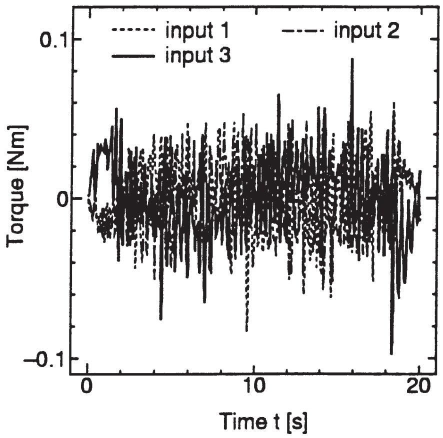

Figure 18. Input torque for a circular path.

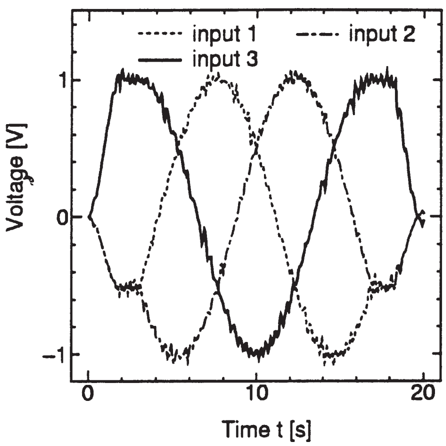

Figure 19. Input voltage for a circular path.

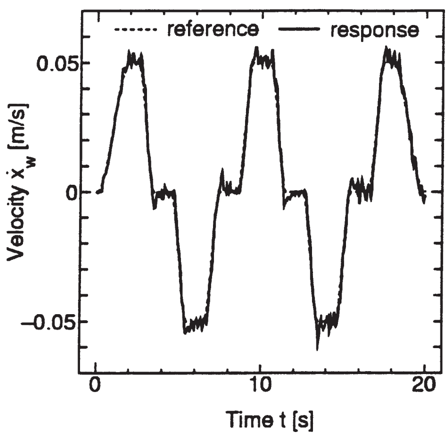

Figure 20. Velocity $\dot{x}_w$ for an 8 character path.

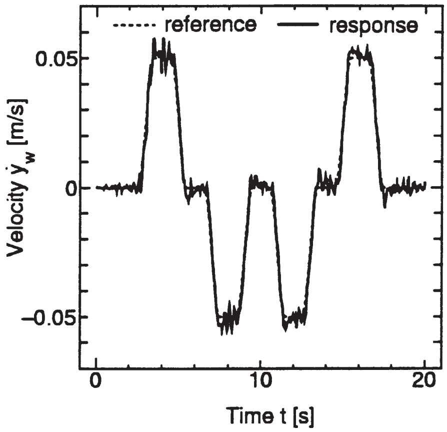

Figure 21. Velocity $\dot{y}_w$ for an 8 character path.

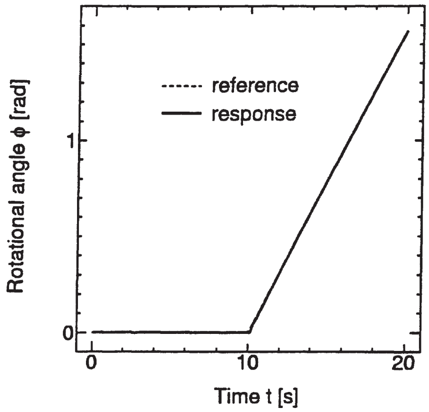

Figure 22. Rotational angle ϕ for an 8 character path.

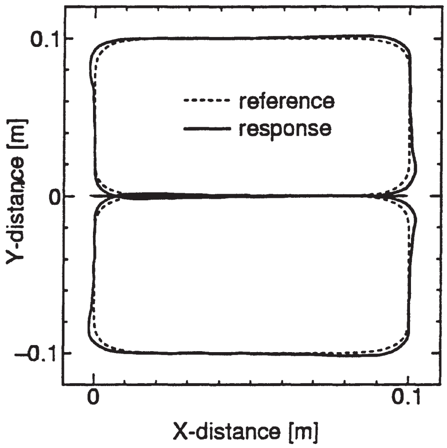

Figure 23. Trajectory for an 8 character path.

in the responses of $\dot{x}_w$ and $\dot{y}_w$, though the response of rotational angle tracks the reference very well. This seems to be attributed to the fact that the time required for the acceleration and deceleration is too short, and in fact it was not improved even if the gains for $\dot{x}_{w\mathrm{d}}$ and $\dot{y}_{w\mathrm{d}}$ were increased.

Furthermore, it should be noted from Figure 22 that the tracking errors appear at the corners of the squared path. It is worth, however, to note that the time-varying or time-invariant property of the rotational angle ϕ does not affect the trajectory response, because the responses on the upper and bottom squared paths are approximately symmetric with respect to the x-coordinate. A compensation approach, such as a sliding mode control for the resolved acceleration control system with a modeling error, may be needed to improve the control response.

6. Conclusions

In this paper, we have derived a dynamic model for an omnidirectional holonomic mobile robot, whose platform was assumed to be based on three lateral orthogonal-wheel assemblies. Then, the resolved acceleration control system was derived using such a model, and several experimental results were presented showing that the present control system was effective for controlling such a mobile robot.

We refer to [12] for the control results through the stochastic fuzzy control approach. See also [13] for the detailed construction problem of the omnidirectional mobile robot using some orthogonal wheel mechanisms.

Representative examples of mobile health-care service robot prototypes (design, implementation, control, human-robot interfacing, operation) can be found in [14–20].

References

1. Nakano, E. and Koyachi, N.: An advanced mechanism of the Omni-Directional Vehicle (ODV) and its application to the working wheelchair for the disabled, in: *Proc. of '83 Int. Conf. on Advanced Robotics*, 1983, pp. 277–284.
2. Nakano, E., Mori, Y., and Takahashi, T.: Study of the mechanism and control of Omni-Directional Vehicle, in: *Proc. of the 12th Annual Conf. of RSJ* 1, 1994, pp. 369–379 (in Japanese).
3. Wada, M., Tominaga, Y., and Mori, S.: Design of an omnidirectional holonomic vehicle, in: *Proc. of the 13th Annual Conf. of RSJ* 1, 1995, pp. 145–146 (in Japanese).
4. Muir, P. F. and Neuman, C. P.: Kinematic modeling of wheeled mobile robots, *J. Robotic Systems* **4** (1987), 281–340.
5. Asama, H., Bogoni, L., Sato, M., Kaetsu, H., and Endo, I.: Kinematics of an omnidirectional mobile robot with 3-DOF decoupling drive mechanism, in: *Proc. of the 12th Annual Conf. of RSJ* 1, 1994, pp. 367–368 (in Japanese).
6. Nishikawa, A., West, M., and Asada, H.: Development of a holonomic omnidirectional vehicle and an accurate guidance method of the vehicles, *J. of the Robotics Society of Japan* **13**(2) (1995), 249–256 (in Japanese).
7. Hirose, S. and Amano, S.: The VUTON: High payload, high efficiency holonomic Omni-Directional Vehicle, in: *Proc. of JSME Annual Conf. on Robotics and Mechatronics*, 1993, pp. 350–355 (in Japanese).
8. Hirano, T., Chen, P., and Toyota, T.: A fundamental study on omnidirectional vehicle (1) – Omnidirectional running mechanism for offroad, in: *Proc. of the 14th SICE Kyushu Branch Annual Conf.*, 1995, pp. 273–274 (in Japanese).
9. Pin, F. G. and Killough, S. M.: A new family of omnidirectional and holonomic wheeled platforms for mobile robots, *IEEE Trans. Robotics Automat.* **10**(2) (1994), 480–489.
10. Iwatsuki, M., Nakano, K., and Ohuchi, T.: Target point tracking control of robot vehicle by fuzzy reasoning, *Trans. of the Soc. Instrum. Control Engineers (SICE)* **27**(1) (1991), 70–76 (in Japanese).
11. Saito, M. and Tsumura, T.: Collision avoidance among multiple mobile robots – A local approach based on nonlinear programming, *Trans. of the Institute of Systems, Control and Information Engineers* **3**(8) (1990), 252–260 (in Japanese).

12. Tang, J., Nomiyama, A., Watanabe, K., and Yubazaki, N.: Stochastic fuzzy control for an autonomous mobile robot, in: *Proc. of the 1996 IEEE Int. Conf. on Systems, Man and Cybernetics*, 1, Beijing China, 1996, pp. 316–321.
13. Tang, J., Watanabe, K., and Shiraishi, Y.: Design of traveling experiment of an omnidirectional holonomic mobile robot, in: *Proc. of the 1996 IEEE/RSJ Int. Conf. on Intelligent Robotics and Systems (IROS '96)*, 1, Osaka, Japan, 1996, pp. 66–73.
14. Klafter, R. D.: Mobile robots, research and development, in: R. C. Dorf and S. Y. Nof (eds), *Internat. Encyclop. of Robotics: Applications and Automation*, Wiley, New York, 1988, pp. 920–943.
15. Kimura, I. and Tadano, J.: Guide and carry robot for hospital use, *Advanced Robotics* **3**(3) (1989), 213–220.
16. Kawamura, K. and Iskarous, M.: Trends in service robots for the disabled and the elderly, in: *Proc. of the 1994 Int. Conf. on Intelligent Robots and Systems (IROS '94)*, Munich, Germany, 1994, pp. 1647–1654.
17. WORKSHOP WS3: Robots for the disabled and elderly people, in: *Proc. 1995 Int. Conf. on Robotics and Automation*, Nagoya, Aichi, Japan, 1995.
18. Rembold, U., Dillmann, R., Hertzberger, L. D., and Kanade, T. (eds): *Intelligent Autonomous Systems*, IOS Press, Amsterdam/Oxford, 1995.
19. Fischer, C., Buss, M., and Schmidt, G.: Hierarchical supervisory control of a service robot using human-robot interface, in: *Proc. of the 1996 Int. Conf. on Intelligent Robots and Systems (IROS '96)*, Osaka, Japan, 1996, pp. 1408–1416.
20. Tzafestas, S. G., Koutsouris, D., and Katevas, N.: *Mobile Robotics Technology for Health-Care Services* (*Proc. of the 1st EEC-TIDE MobiNet Symp.*), Athens, May, 1997.